References and Notes

1. W. J. Morgan, *J. Geophys. Res.* **73**, 1959 (1968); X. LePichon, *ibid.*, p. 3661; B. Isacks, J. Oliver, L. R. Sykes, *ibid.*, p. 5855; F. J. Vine and H. H. Hess, in *The Sea*, E. C. Bullard, E. Goldberg, J. L. Worzel, Eds. (Interscience, London, in press), vol. 4 (preprint, 1969).
2. P. B. King in *Zoogeography*, C. L. Hubbs, Ed. (AAAS, Washington, D.C., 1958), p. 3; J. D. Love, *Amer. J. Sci.* **258A**, 204 (1960); F. B. Van Houten, *ibid.* **259**, 612 (1961); L. G. Morales, and The Colombian Petroleum Industry, in *Habitat of Oil*, L. G. Weeks, Ed. (Amer. Ass. Petrol. Geol., Tulsa, Oklahoma, 1958), pp. 641–695; F. B. Van Houten and R. B. Travis, *Bull. Amer. Assoc. Petrol. Geol.* **52**, 675 (1968).
3. H. Füchtbauer, *Eclogae Geol. Helv.* **57**, 157 (1964); M. Gignoux, *Stratigraphic Geology* (Freeman, San Francisco, 1955), pp. 564–567.
4. A. Gansser, *Geology of the Himalayas* (Interscience, London, 1964), pp. 45–54, 80–85, 146, 174–175; D. N. Wadia, *Geology of India* (MacMillan, London, 1953), pp. 263–275.
5. J. Aubouin, *Geosynclines* (Elsevier, Amsterdam, 1955), pp. 34, 37, 66, 96, 105, 192, 218–219. Molasse troughs may also be considered as simply a continuation of geosynclinal deformation, involving only further migration toward the craton. Use of the term "molasse trough" emphasizes its distinctive features and development.
6. H. W. Menard, *Sci. Amer.* **205**, No. 6, 52 (1961); K. L. Cook, *Geol. Soc. Canada, Pap. No. 66–14* (Geol. Soc. Canada, Ottawa, 1965), pp. 246–279.
7. X. LePichon, *J. Geophys. Res.* **73**, 3681 (1968); F. J. Vine and H. H. Hess, *ibid.*, p. 33.
8. X. LePichon, *ibid.*, p. 3685; F. J. Vine and H. H. Hess, *ibid.*, p. 29.
9. R. S. Yeats, *Bull. Geol. Soc. Amer.* **79**, 1693 (1968).
10. F. J. Vine, *Science* **154**, 1405 (1966).
11. R. L. Larson, H. W. Menard, S. M. Smith, *ibid.* **161**, 781 (1968).
12. H. Bürgl, *Tectonophysics* **4**, 440 (1967). W. E. Nygren, *Bull. Amer. Ass. Petrol. Geol.* **34**, 1998 (1950).
13. E. M. Herron and J. R. Hiertzler, *Science* **158**, 775 (1967).
14. X. LePichon, *J. Geophys. Res.* **73**, 3691 (1968).
15. A. Gansser, *ibid.*, pp. 253, 256–261; A. Holmes, *Principles of Physical Geology* (Ronald Press, New York, 1965), p. 1100.
16. B. Isacks, J. Oliver, L. R. Sykes, *J. Geophys. Res.* **73**, 5855 (1968).
17. W. J. Morgan, *ibid.*, p. 1959, Fig. 1.

18 August 1969

Visual Pigment Density in Single Primate Foveal Cones

Abstract. *The feasibility is demonstrated of microspectrophotometric studies on primate photoreceptors aligned at right angles to the test beam, rather than axially illuminated. Pigment densities, and hence absorption per unit thickness, are approximately equal in primate rods and foveal cones. These pigment densities are similar to those reported for frog rods and fish cones.*

Microspectrophotometric studies demonstrated the existence of three visual pigments, isolated in separate cones, in both fish (*1–3*) and primates (*4–6*). These experiments elucidated the physiological basis for the trichromacy of vision and provided direct experimental confirmation of the Young-Helmholtz theory.

In the teleost experiments, teased preparations of receptors lying on their sides were employed, while the small size of primate cones dictated axial illumination to maximize the ratio of signal to noise. In addition to being the physiological orientation, the mosaic arrangement of receptors on end also simplifies differentiation of rods and cones and offers the possibility of studying the topographical relations among receptor types.

However, optical quality of the microscope objectives must be sacrificed to obtain the necessary long working distances. The preparation is also inconvenient both because suitable patches of retina are rarely located near an open area through which the reference beam of our microspectrophotometer can pass and because otherwise suitable receptors are usually observed leaning at an angle to the optical axis of the instrument.

Most serious of all, the intervening neural layers complicate the optical path, and scatter increases with clouding after death. This scatter causes the spectrum to be contaminated by the absorbtion of surrounding rods and is partially offset by the focusing effect of the inner segments of the cone. Estimates of pigment concentration in primate cones were thus complicated by the fact that the intensity of illumination of all points along the receptor outer segment was unknown.

On the other hand, the clearly defined optical geometry of the side-illuminated configuration permitted estimation of the absorption to be about 1.8 percent/μ of thickness (*1, 3*) in both frog rods and fish cones. Liebman's (*2*) absorptions are higher, probably because of less scatter. Calculations indicated that, under optimal conditions, it should also be possible to study primate receptors oriented at right angles to the optical axis. This method appears to be the only one applicable to the study of primate foveal cones since they are about 0.8 μ in diameter and densely packed. It does not appear feasible at this time to confine an axial beam of illumination to a single receptor of this type. However, the extinction of a cone lying on its side is far less than that of the same receptor on end, and the signal is further diluted by any light scattered around the outer segment. Consequently, ratios of signal to noise are critical (*7*), and further refinements were therefore made in the previously reported (*3*) instrument and technique.

Suitable field diaphragms were fabricated by milling slits in soft brass with a "flycutter." These slits were approximately 60 μ wide, and their length was adjusted by masking the ends with black tape. At the specimen plane they are projected at a width of about $\frac{2}{3}$ μ (Fig. 1).

The geometric problems of superimposing the image of a slit (rather than a pinhole) on a cylindrical receptor necessitated installation of a "sliding-gliding" stage (Zeiss). This stage permits extremely fine adjustments as well as rotation to examine any receptor, regardless of its original orientation in the field of view.

Because of the orientation of the visual pigment molecules in the lamellae of photoreceptors, polarized light was used on primate cones, as described earlier for goldfish receptors (*1, 3*). The increase in the ratio of signal to noise was substantial and approximated the factor of $2\frac{1}{2}$ predicted on theoretical grounds.

Alignment of the machine is critical. Virtually imperceptible adjustments in the focus of the monochromator filament on the back focal plane of the condenser can change the slope of the base line by a factor of 10.

Other efforts to refine the optical system concentrated on reducing longitudinal and lateral chromatic aberration to a minimum, and tests were run on more than 100 selected objectives (*8*).

Longitudinal chromatic aberration, the change in focal length with wavelength, can be easily observed in the spectrophotometer by scanning through the spectrum and watching the focus of the test and reference beams change. With paired optics for condenser and objective, measurements were made by refocusing at 25-nm intervals and recording adjustments from the fine-focus micrometer.

Lateral chromatic aberration, the change in magnification with wavelength, is manifested by lateral movements of the test beam so that the beam no longer passes through the receptor. This effect was evaluated by measurement of magnification changes on Polaroid photographs taken with different wavelengths and can be as much as 3 μ.

The effects of longitudinal chromatic

aberration can be further minimized by decreasing numerical aperture. This is accomplished most effectively at the back focal plane of the condenser. Unfortunately, in most modern optics this focal plane is located at a cemented surface and hence is not accessible; however, appropriate iris diaphragms are found in a number of oil immersion objectives designed for dark-field work. Simultaneously, the effects of lateral chromatic aberration can be minimized by placing the test beam on the optical axis of the instrument, in which case its dimensions may change slightly but gross movements away from the receptor are eliminated.

A Zeiss 40× immersion apochromat with built-in iris diaphragm (stopped down to 0.6) was chosen for the condenser. Many differing lenses were used as objectives. The prime function of this second lens is simply to collect the light passing through the receptor; its image-forming qualities are less critical.

Many problems with the preparation are eliminated by the change in configuration. In addition to obviating optical complications due to the intervening neural tissue and inner segments, mounting intricacies of teased preparations are negligible, and damage to the outer segments can be easily observed. Difficulties in finding clear areas for the reference beam are eliminated and, because the preparations are thin, they are less subject to mechanical and thermal changes. Consequently, they last much longer, and a number of receptors can be examined from any given retina.

Certain orientation problems are, however, introduced. Receptors tend to curve slightly, and, despite efforts to orient them by "streaking" techniques, only segments less than 10 μ in length could be reliably superimposed on the image of a straight slit. In addition, it is difficult to differentiate rod and cone outer segments, particularly when the inner segments are broken off. Consequently, experiments were restricted to those receptors in which the inner segments were clearly visible or to preparations confined to the center of the fovea. This was facilitated by experience in dissection and preparation of over 500 human and monkey retinas.

Gelatin had been employed in the original experiments to stabilize the position of the receptors in the optical system; however, different lots of gelatin vary tremendously in optical and mechanical properties. Numerous natural and synthetic gels and viscous liquids, including methylcellulose and low-methyl pectins were therefore investigated as a replacement. The problems of clarity and mechanical stability were finally overcome by obtaining a supply of high purity 285 Bloom gelatin (*9*). This was prepared as an 8 percent solution with buffered mammalian Ringer solution. Special cover slips for use with

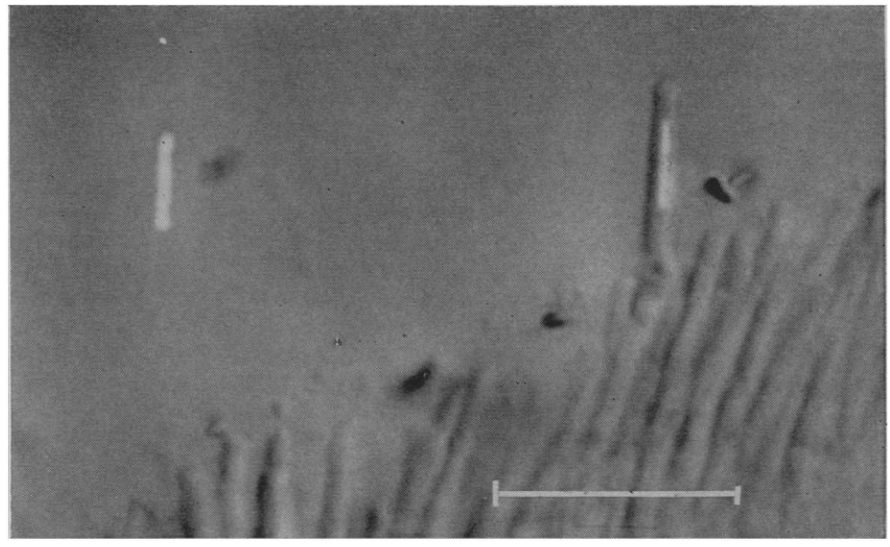

Fig. 1. Human foveal cone oriented at right angles to the optical axis of the microspectrophotometer. The receptor is trans-illuminated by the test beam while the reference channel passes through a tissue-free area. The proximity of adjacent receptors illustrates the necessity of orienting foveal cones at right angles to the optical axis. Scale, 10 μ.

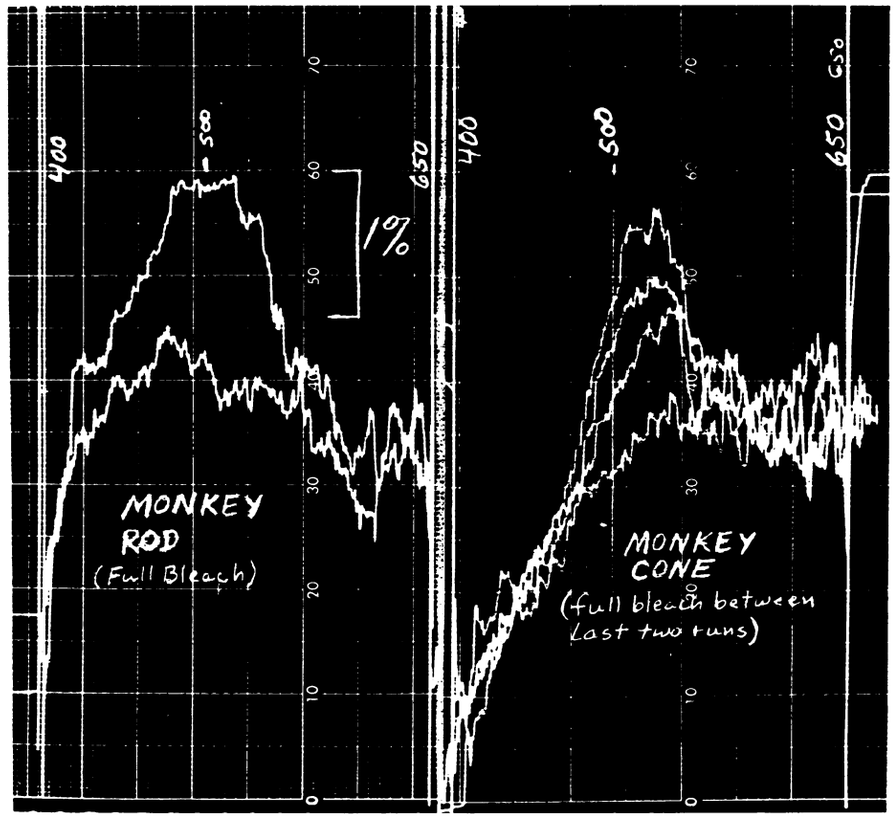

Fig. 2. Records obtained from a parafoveal rod and foveal cone oriented at right angles to the optical axis of the microspectrophotometer. Both spectra were recorded from the same *Macaca nemestrina* retina. Pigment densities from all receptors seemed similar, if they had not been inadvertently bleached in handling.

precision optics were employed (Corning, No. 1½).

Much of the tendency of slides to deteriorate over a period of a few hours was traced to evaporation through pinhole imperfections in the wax used to seal the preparation. This was eliminated by using two cover slips of unequal size creating a shoulder on which the wax could bind, and by using a mixture of one part Vaseline to three parts paraffin instead of pure paraffin.

Although the effect of each of the above refinements is small, they combine to permit recording from primate cones lying on their sides. No changes were necessary in the electronics.

Several hundred foveal and parafoveal primate cones (mostly human) have been examined oriented at right angles to the measuring beam in the course of developing these refined techniques. Ratios of signal to noise have been very poor until the series shown in Fig. 2; these are the best records which have been obtained so far and demonstrate the feasibility of the technique.

Each receptor is about 0.8 μ in diameter and absorbs about 1.3 percent at maximum. The pigment density in primate rods and cones is similar and is in turn comparable to the densities (*1, 3*) for frog rods and fish cones. With a specific absorption of 1.8 percent/μ, the total absorption of a foveal cone 45 μ in length would be about 50 percent. This probably represents a lower limit due to light scattered around the receptor. Psychophysical experiments (*10, 11*) have indicated that the maximum absorption may be in excess of 80 or 90 percent. However, too few successful preparations were obtained to determine the relative numbers of cones of each spectral class, or to confirm earlier measurements (*4, 5*) of the maximum absorption of each class.

W. H. DOBELLE,* W. B. MARKS
E. F. MACNICHOL, JR.†
Thomas C. Jenkins Department of Biophysics, Johns Hopkins University, Baltimore, Maryland

References and Notes

1. W. B. Marks, thesis, Johns Hopkins University (1963).
2. P. A. Liebman, *J. Opt. Soc. Amer.* **54**, 1451 (1964).
3. W. B. Marks, *J. Physiol.* **178**, 14 (1965).
4. ——— W. H. Dobelle, E. F. MacNichol, Jr., *Science* **143**, 1181 (1964).
5. P. K. Brown and G. Wald, *Science* **144**, 45 (1964).
6. W. H. Dobelle, thesis, Johns Hopkins University (1967).
7. The signal-to-noise ratio is approximately equal to the height times the square root of the area. Therefore, $\frac{\text{end-on}}{\text{side}} \approx \frac{30\,(0.8)^{\frac{1}{2}}}{0.8\,(10)^{\frac{1}{2}}} \approx$ tenfold decrease in the ratio of the signal to noise.
8. The objectives were furnished by Zeiss, Leitz, Zeiss-Jena, Wild, Bausch and Lomb, American Optical, and Nikon.
9. Samples of all embedding media were originally supplied by Sunkist Laboratories, Box 2706, Los Angeles, California 90054. The gelatin is no longer available. However, extremely transparent 300 Bloom (a measure of viscosity) gelatin is presently produced by Swift and Co., 1211 W. 22nd St., Oak Brook, Illinois 60521.
10. G. Brindley, *Proc. Phys. Soc.* (*London*) **68B**, 862 (1955).
11. P. L. Walraven, thesis, University of Utrecht (Institution for Perception RVO-TNO) Soesterberg, Netherlands (1962).
12. Supported by NSF grant GB-2705 and NIH grant NB-03582. Direct reprint requests to Building 512, University of Utah, Salt Lake City 84112.
* Present address: Joint program of Departments of Physiology and Computer Sciences and Division of Artificial Organs, University of Utah, Salt Lake City 84112.
† Present address: National Institute of Neurological Diseases and Stroke, Bethesda, Maryland 20014.

23 July 1966; revised 22 August 1969

Imidodiphosphate and Pyrophosphate: Possible Biological Significance of Similar Structures

Abstract. *The structure of sodium imidodiphosphate has been determined by single crystal x-ray diffraction. The P–N–P bond angle (127.2°) and P–N bond distance (1.68 angstroms) are remarkably similar to newly refined values for the P–O–P bond angle (128.6°) and the bridging P–O bond distance (1.63 angstroms) of sodium pyrophosphate. This close similarity may explain why P–N–P linkages in algal "polyphosphates" escaped detection until recently and why adenosine triphosphate analogs with this linkage mimic adenosine triphosphate so closely.*

Correll (*1*) has found imidodiphosphate (P–N–P) linkages in algal "polyphosphate." This is the first instance of P–N–P linkages being observed in a natural product. Almost nothing is known of the metabolism of P–N–P compounds, but knowledge of the molecular dimensions of the P–N–P linkage should aid in these studies. In addition, an adenosine triphosphate (ATP) analog in which an imidodiphosphate grouping replaces the terminal pyrophosphate has been synthesized (*2*). Correll's finding and the striking similarity of this analog to ATP in binding to contractile proteins (*2*) led us to investigate the crystal and molecular structure of sodium imidodiphosphate in relation to that of sodium pyrophosphate.

Crystals of tetrasodium imidodiphosphate·decahydrate were prepared according to Nielsen *et al.* (*3*). The crystals were monoclinic, with space group $C2/c$ and cell dimensions $a = 17.069$, $b = 6.905$, and $c = 14.752$ Å, and $\beta = 110.33°$, and were isomorphous with tetrasodium pyrophosphate·decahydrate. The measured density of 1.80 g/cm^3 and the calculated density of 1.812 g/cm^3 indicated that there were four molecules per unit cell. Of the 1065 intensities measured with a Picker diffractometer, 985 were observed above background. The positional parameters and anisotropic thermal parameters were refined by least squares methods (*4*) to an R-index

$$R = \frac{\Sigma\,||F_o| - |F_c||}{\Sigma\,|F_o|}$$

of 0.054. All hydrogen atoms were located on the final electron density map but were not included in the refinement (Table 1; Fig. 1a). There was no evidence for the tautomeric form

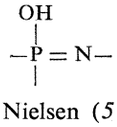

as suggested by Nielsen (*5*). However, the shortened P–N bond distances, 1.68 Å versus 1.77 Å for the single P–N bond distance in $NaPO_3NH_3$ (*6*), indicates at least partial double bond character of the P–N–P linkages.

Table 1. Comparison of the geometries of sodium pyrophosphate, sodium imidodiphosphate, and methylene diphosphonic acid. The standard deviation on the least significant digit is given in parentheses.

Bond	$O(PO_3)_2NA_4 \cdot (H_2O)_{10}$*	$O(PO_3)_2Na_4 \cdot (H_2O)_{10}$	$HN(PO_3)_2Na_4 \cdot (H_2O)_{10}$	$CH_2(PO_3)_2H_4$†
P–X	1.63Å	1.631(7)Å	1.678(5)Å	1.79Å
P–O (ave)	1.48Å	1.512(20)Å	1.521(7)Å	1.54Å
P–P		2.942(16)Å	3.006(3)Å	3.05Å
P–X–P	133.80°	128.7(3)°	127.2(5)°	117°

* Calculated from 246 observed structure factors using zonal data refinement ($R = 0.22$) (*7*).
† See (*15*).